

# Delamination and Failure at Ply Drops in Carbon Fiber Laminates Under Static and Fatigue Loading

Daniel D. Samborsky\*, Darrell P. Avery†, Pancasatya Agastra‡ and John F. Mandell‡

*Department of Chemical and Biological Engineering, Montana State University, Bozeman, MT, 59717, USA*

**Delamination at ply drops in composites with thickness tapering has been a major concern in aerospace applications of carbon fibers, where the plies are typically very thin. This study explored the resistance to delamination in fatigue of hybrid carbon fiber and glass fiber prepreg laminates containing various ply drop geometries, and using thicker plies typical of wind turbine blades. Strain levels to produce significant delamination at both carbon and glass fiber ply drops were determined and compared in terms of a simple delamination model. The carbon fiber laminates with ply drops, while performing reasonably well under static loads, delaminated in fatigue at low maximum strain levels except for the thinnest ply drops. The lower elastic modulus and higher interlaminar toughness of the glass fiber prepreg resulted in much higher strains to produce delamination at equivalent ply drops, compared with carbon fiber prepreg using the same resin system. The results indicate that the thickness of ply drops with carbon fibers should be much less than those commonly used for glass fibers.**

## I. Introduction

The primary structural elements in most wind turbine blades are spars with tapering thickness along their length. Thickness tapering in laminated composites is accomplished by a series of terminations of individual plies or groups of plies, called ply drops. When loads are applied to a blade, these ply drops cause stress concentrations in adjoining plies and can also serve as an initiation site for the separation, or delamination, of the plies. Ply delamination, if widespread, can cause a general loss in structural integrity of the blade. Delamination and ply drops have received extensive attention in the general composites literature<sup>1-5</sup> and, to a lesser extent, in wind turbine blade technology.<sup>6,7</sup> Methodologies for predicting delamination under static and fatigue loading using finite elements have been demonstrated.<sup>4,6</sup> Recent attention has been given to this problem in the aerospace community in the area of tapered flex beams for helicopter rotors.<sup>8,9</sup>

The ply drop problem is of particular concern for wind turbine blades using carbon fibers for three reasons: first, the more directional elastic constants of carbon fiber laminates often increase the tendency to delaminate relative to glass; second, to reduce cost, the plies are often thicker in composites for wind turbine blades relative to aerospace applications; and third, the ultimate and fatigue strains in compression for lower cost forms of carbon fiber laminates are lower than for glass,<sup>10,11</sup> and may be design drivers in some cases. Thus, while ply drops may not have been a major problem for glass fiber blades, they may prove critical with carbon fibers.

The study reported here has concentrated on exploring the strain levels for delamination and/or gross failure with several variations, including carbon vs. glass fibers, ply drop location through the thickness, number of plies dropped at one location (simulating changes in ply thickness), laminate thickness, and loading conditions (tension, compression and reversed loading.) While fracture mechanics based methodology is available to predict delamination growth under defined conditions,<sup>4,6</sup> the most useful data for material selection and design of wind turbine blades is in the form of stress and strain levels to produce significant delamination, which doesn't require complex analysis.

---

\*Research Engineer, ChBE Department, 306 Cobleigh Hall, Bozeman, MT, 59717, Not a member.

† Graduate Student, ChBE, 306 Cobleigh Hall, Bozeman, MT, 59717, Not a member.

‡ Professor, ChBE, 306 Cobleigh Hall, Bozeman, MT, 59717, Senior Member.

## II. Background

This study was preceded by an exploratory study of ply drops in carbon/glass hybrid laminates processed by both prepreg and hand lay-up molding.<sup>10</sup> The laminates contained 0° carbon fiber plies and ±45° glass fiber plies, where 0° is the uniaxial load direction. All tests were static compression. The position and number of ply drops and ply joints was varied; 0° carbon ply thicknesses were about 0.33 mm for the prepreg and 1.0 mm for the hand lay-up fabrics.

The results of these tests<sup>10</sup> were that compression strength and ultimate compression strain were reduced moderately for both material systems for a single ply drop or joint, to an ultimate compression strain of about 0.7% for the best prepreg ply drop positions, slightly lower for the hand lay-up laminates. Double ply drops at the same position for the prepreg reduced the ultimate compressive strain values to 0.44 and 0.54% depending on ply drop position. Results were similar whether plies were dropped at mid-thickness of the 0° ply stack or on the surface of the stack, under the ±45° layers.

Failure modes for the ply drop coupons did not indicate any stable delamination growth prior to gross compressive failure. However, earlier studies<sup>6</sup> of glass laminates had shown a shift to delamination prior to gross failure under fatigue loading. Such a shift could potentially cause an increase in slope of the S-N fatigue curve compared to coupons without ply drops, as the delamination process is strictly a matrix/interface failure.

## III. Experimental Methods

### A. Materials

Three different prepregs, supplied by Newport Adhesive and Composites, Inc, were used in this study. Two unidirectional prepregs: carbon (NCT307-D1-34-600-G300) and E-glass (NCT307- D1-E300), and one E-glass 0/90 woven fabric (NB307-D1-7781-497A) orientated at 45° for ±45 plies. All three prepregs employed the same epoxy resin system. All the test laminates utilized external ±45 glass plies. Plies were cut from the prepreg roll and individually laminated together using a rubber roller. To facilitate the tapering thickness of the laminate at the ply drops, sacrificial plies of the same prepreg type and number of dropped plies, were placed in the dropped regions, separated from the ply drop laminate by a Teflon sheet (See Reference 10). This allowed the use of simple flat and parallel caul plates. The prepreg was cured for 3 hours at 121°C in a vacuum bag with a vacuum of 75 kPa.

Thin laminates (<4 mm thick) in the base configuration (±45/0<sub>9</sub>/±45) were used for exploratory tests under tensile, compressive, and reversed fatigue loading. Thicker laminates, [(±45)<sub>3</sub>/0<sub>27</sub>/(±45)<sub>3</sub>] (10 – 13 mm thick) were used for the main study, subjected only to compressive loading.

Additional 3 mm thick fiberglass G10 tabs were bonded to the test coupons with Hysol 9309.2 NA epoxy and cured for two hours at 60°C. Test coupons were sized so that the length of coupon would fit to the hydraulic wedge grip pistons to allow for end loading. A photo of a typical ply-drop specimen is shown in Figure 1, along with a schematic giving specimen dimensions.

### B. Mechanical Testing and Data Reduction

Mechanical testing was performed in Instron 8501 and 8802 servo-hydraulic test machines with capacities of 100 and 250 kN respectively. The static (1-cycle) tests were performed under displacement control with a linear ramp rate of 13 mm/s, which produced a similar loading rate to the fatigue tests. The fatigue tests were performed under load control with a sinusoidal waveform with frequencies between 1 and 6 Hz.

Compression tests of the thin laminates with no ply drops used 25 mm wide rectangular specimens having a gage length of 13 mm, with no lateral constraint on the gage section. Thicker laminates (10 - 13 mm) and the thin laminates with a ply drop used a 25 mm gage length. In all cases, the coupons were monitored for buckling. Specimens were held in hydraulic grips with special anti-rotation and anti-deflection restraints.<sup>12</sup> These were needed for both testing machines, as they employ hydrostatic bearings, which allow some lateral grip movement. Compression tests are designed and validated for materials based failure without elastic buckling.

Compressive stress-strain curves were generated from specimens without ply drops to obtain modulus values which were used to calculate strain values from the stress determined in the tests. All stresses and strains in the results represent the thin side of the ply drop specimens.

Ply properties for each type of prepreg were obtained using standard test methods described in Reference 12. Fatigue S-N curves for laminates without ply drops were obtained on (±45/0<sub>8</sub>/±45) coupons molded and tested as described above, with a 13 mm gage length.

Interply delamination resistance in Modes I and II ( $G_{IC}$  and  $G_{IIC}$ ) used unidirectional 0° double cantilever beam (DCB) and end notched flexure (ENF) test specimens.<sup>12</sup> These specimens included a Teflon crack-starter strip

embedded during fabrication as an initial crack. The  $G_{IC}$  and  $G_{IIC}$  values were determined from the initial crack growth from the starter strip, which provides the most conservative value for most wind turbine blade laminates.<sup>12</sup>

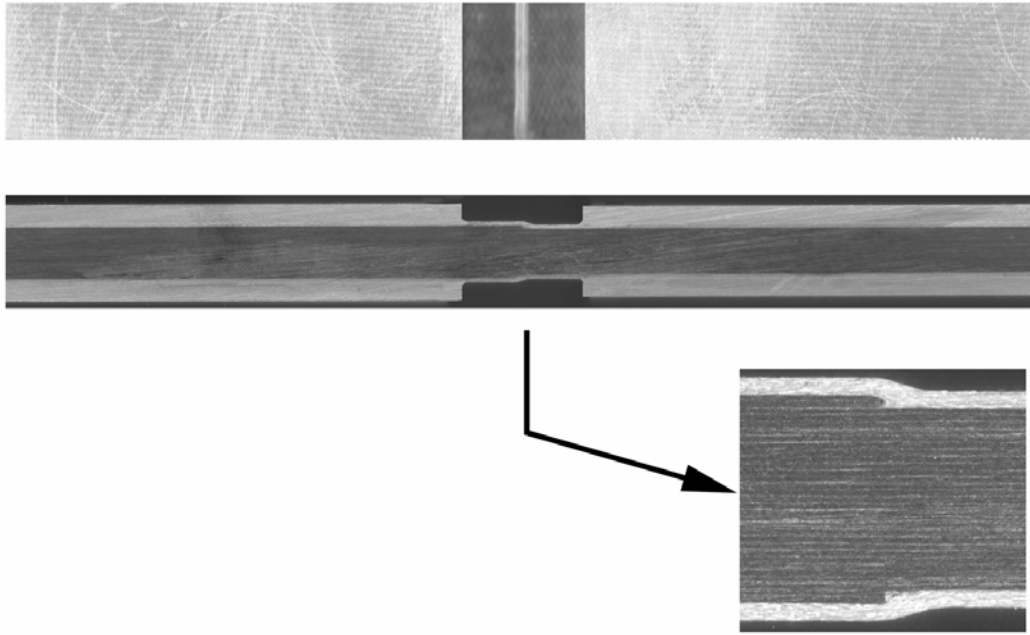


Figure 1. Schematic and Photo of Typical Ply Drop Coupon (Two Plies Dropped at Surface of  $0^\circ$  Stack)

#### IV. Results and Discussion

##### A. Thin Laminates

The thinner the laminate is, the less complex are the test methodology and failure modes. However, since laminates contain plies with a fixed ply thickness, ply drops in thin laminates are not representative of thick blades in terms of the fraction of plies dropped at a particular cross-section. Thus, a series of relatively thin laminates, on the order of 3 mm thick, was tested both with and without ply drops under tensile, compressive, and reversed loading ( $R = 0.1, 10, \text{ and } -1.0$ , where  $R$  is the ratio of minimum to maximum stress, with compression negative). The results were then compared with data given later from relatively thick laminates for selected cases where meaningful tests could be run. The ply configuration for the thin laminates was  $(\pm 45/0_9/\pm 45)$ , with additional plies added for half of the coupon length in the case of ply drops. As noted earlier, the  $0^\circ$  plies contained carbon fibers, while the  $\pm 45^\circ$  plies contained glass fibers ( $0^\circ$  is the uniaxial load direction).

S-N fatigue curves for coupons without ply drops were reported in Reference 11 for this material system, for the similar ply configuration  $(\pm 45/0_8/\pm 45)$  with the three  $R$ -values. Figures 2 and 3 give these control fatigue data in terms of absolute maximum stresses and strains, respectively. Table 1 gives measured ply properties for these prepreps.

The results for the thin laminates containing ply drops,  $(\pm 45/0_2^*/0_9/0_2^*/\pm 45)$ , where the  $0_2^*$  plies are dropped at mid-length, are given in Figures 4 and 5. The two double ply drops reduce the static strengths by approximately 45% in tension and 42% in compression (Table 2). These reductions for double ply drops are slightly less severe than those reported for a different prepreg system in Reference 10. However, as feared, the effects of ply drops on the fatigue life are severe, producing much steeper S-N curves than for the controls (Figures 2 and 3). Failure is taken as the growth of a large (6 mm) delamination or combined delamination and separation. Delamination is a matrix failure mode which follows a steeper S-N trend than do control laminates which are more fiber dominated.<sup>13</sup> Maximum strain levels for  $10^6$  cycles are below 0.3% for the laminates with double ply drops, compared with 0.6% to 1.0% for the control material, depending on  $R$ -value. As with the control material, reversed loading is most severe.

It is noteworthy that all three loading conditions produce delamination in a similar strain range. Since a change from tension to compression changes the opening mode delamination from opening to closing, where closing would

suppress delamination, this implies that delamination is dominated by the Mode II, or shear component, as discussed later.

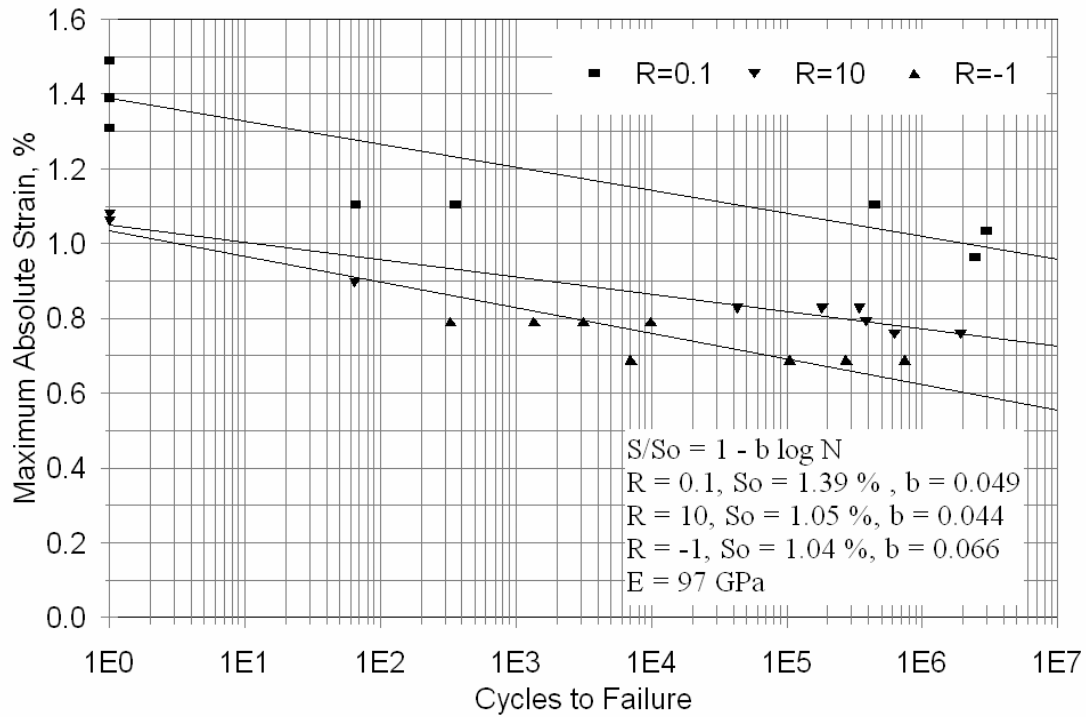


Figure 2. Control Fatigue Maximum Absolute Strain to Failure Data for  $[\pm 45/0_g/\pm 45]$  Laminate,  $R=0.1, 10$  and  $-1$  (No Ply Drops;  $0^\circ$  plies are carbon,  $\pm 45^\circ$  plies are glass).

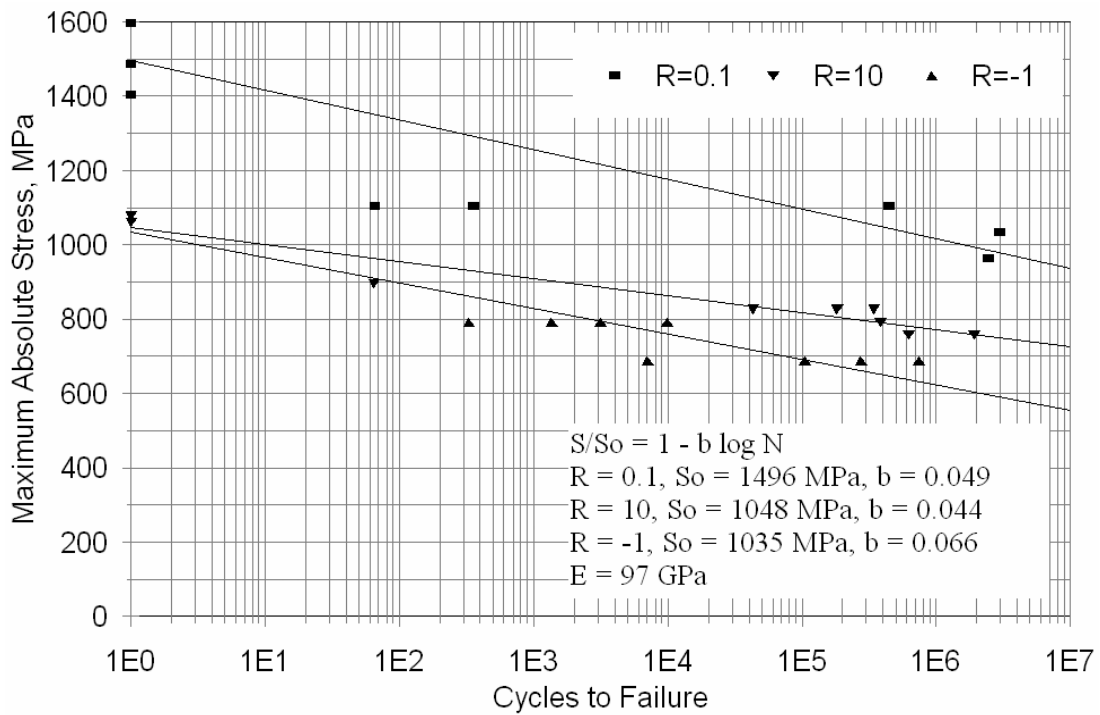


Figure 3. Control Fatigue Maximum Absolute Stress to Failure Data for  $[\pm 45/0_g/\pm 45]$  Laminate,  $R=0.1, 10$  and  $-1$  (No Ply Drops;  $0^\circ$  plies are carbon,  $\pm 45^\circ$  plies are glass).

Table 1. Measured Ply Properties and Delamination Resistance in Material Principle Directions for E - Glass and Carbon Prepregs (static longitudinal, transverse, simulated shear and delamination resistance).

			Longitudinal Direction							
			Elastic Constants				Tension		Compression	
Prepreg	lay-up	V <sub>F</sub> %	E <sub>L</sub> GPa	E <sub>T</sub> GPa	ν <sub>LT</sub>	G <sub>LT</sub> GPa	UTS <sub>L</sub> MPa	ε <sub>U</sub> %	UCS <sub>L</sub> MPa	ε <sub>U</sub> %
NB307-D1 7781 497A	0/90	39	19.2	19.2	0.13	4.50	337	2.21	-497	-2.60
NCT307-D1-34-600 Carbon	[0] <sub>10</sub>	53	123	8.20	0.31	5.08	1979	1.32	-1000	-0.90
NCT307-D1-E300 Glass	[0] <sub>10</sub>	47	35.5	8.33	0.33	8.55	1005	2.83	-788	-2.22

Notes: All coupons for this Table were tested at 0.25 mm/s, with a 100 mm gage length. Compression tests used a 13 mm gage length with unsupported edges. E<sub>L</sub> - Longitudinal modulus, ν<sub>LT</sub> - Poisson's ratio, G<sub>LT</sub> and τ<sub>TU</sub> - Shear modulus and ultimate shear stress by ASTM D3518. UTS<sub>L</sub> - Ultimate longitudinal tensile strength, ε<sub>U</sub> - Ultimate strain, UCS<sub>L</sub> - Ultimate longitudinal compressive strength.

			Shear	Transverse Direction			
				Tension		Compression	
Prepreg	lay-up	V <sub>F</sub> %	τ <sub>U</sub> MPa	UTS <sub>T</sub> MPa	ε <sub>U</sub> %	UCS <sub>T</sub> MPa	ε <sub>U</sub> %
NB307-D1 7781 497A	0/90	39	115	337	2.21	-497	-2.60
NCT307-D1-34-600 Carbon	[0] <sub>10</sub>	53	103	59.9	0.76	-223	-2.72
NCT307-D1-E300 Glass	[0] <sub>10</sub>	47	112	51.2	0.74	-168	-2.02

Delamination Resistance*				
Prepreg	Lay-up	V <sub>F</sub> %	G <sub>IC</sub> (J/m <sup>2</sup> )	G <sub>IIC</sub> (J/m <sup>2</sup> )
NCT307-D1-34-600 Carbon	[0] <sub>20</sub>	53	364 (62)	1829 (87)
NCT307-D1-E300 Glass	[0] <sub>20</sub>	47	365 (37)	2306 (188)

\* 13 to 14 tests, Brackets indicate standard deviation.

Table 2. Comparisons of the Static Strengths of Selected Materials, With and Without Ply Drops (0° plies are carbon, ±45° plies are glass).

Lay-up	Ultimate Compressive Strength, MPa	Ultimate Compressive Strain, %	Ultimate Tensile Strength, MPa	Ultimate Tensile Strain, %
(±45/0 <sub>8</sub> /±45)	-1070	-1.04	1496	1.40
(±45/0 <sub>2</sub> */0 <sub>9</sub> /0 <sub>2</sub> */±45)	-617	-0.64	827	0.85
((±45) <sub>3</sub> /0*/0 <sub>27</sub> /0*/(±45) <sub>3</sub> )	-754	-0.78	----	----
((±45) <sub>3</sub> /0 <sub>2</sub> */0 <sub>27</sub> /0 <sub>2</sub> */(±45) <sub>3</sub> )	-642	-0.67	----	----
((±45) <sub>3</sub> /0 <sub>4</sub> */0 <sub>27</sub> /0 <sub>4</sub> */(±45) <sub>3</sub> )	-612	-0.64	----	----

\* indicates dropped ply. All values measured on thin section.

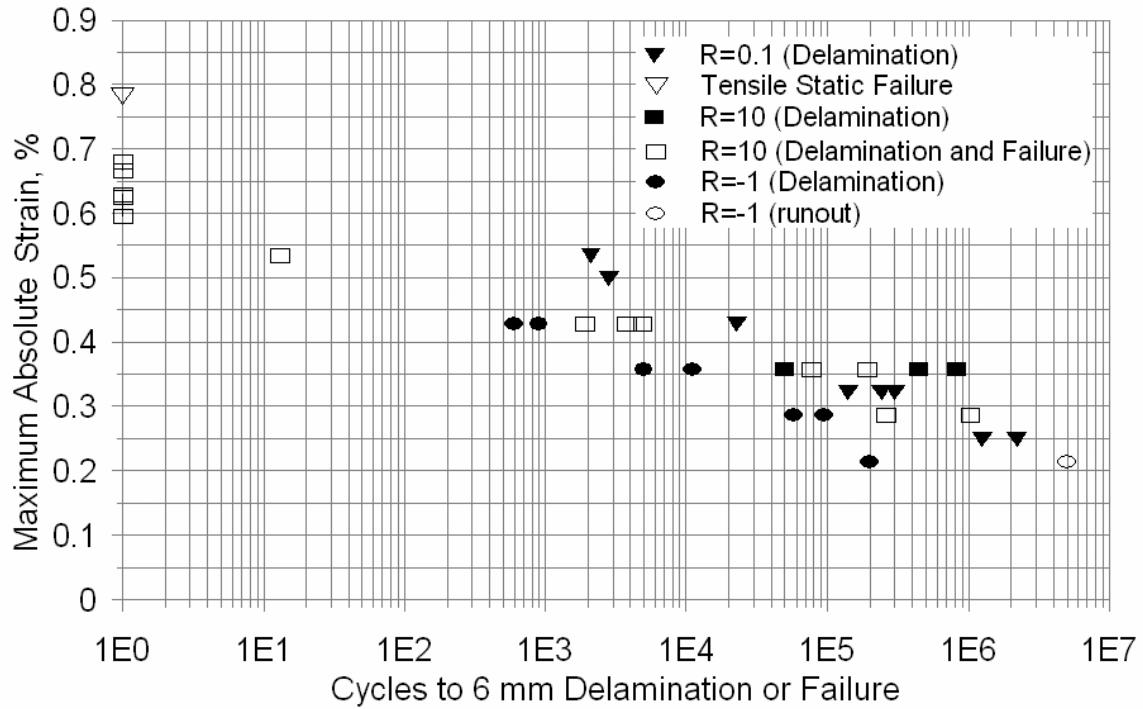


Figure 4. Maximum Absolute Strain versus Cycles to Failure for a  $[\pm 45/0_2^*/0_9/0_2^*/\pm 45]$  Laminate, R=0.1, 10 and -1 (Contains Ply Drops for the  $0_2^*$  Plies;  $0^\circ$  plies are carbon,  $\pm 45^\circ$  plies are glass).

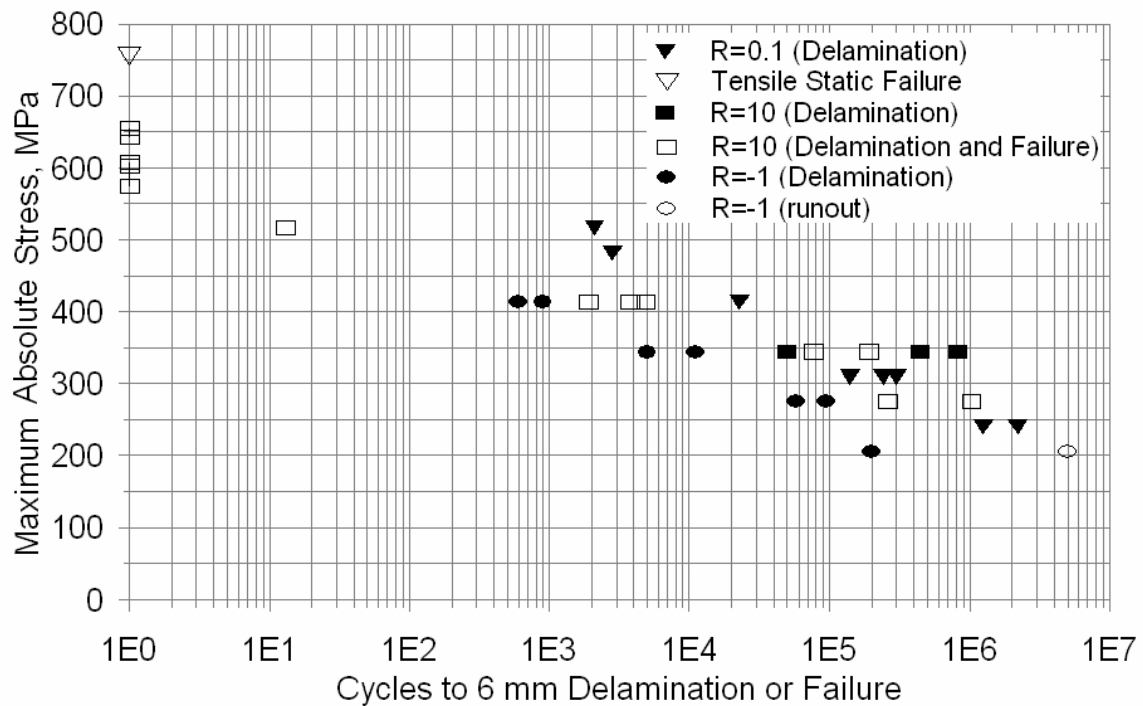


Figure 5. Maximum Absolute Stress versus Cycles to Failure for a  $[\pm 45/0_2^*/0_9/0_2^*/\pm 45]$  Laminate, R=0.1, 10 and -1 (Contains Ply Drops for the  $0_2^*$  Plies;  $0^\circ$  plies are carbon,  $\pm 45^\circ$  plies are glass).

## B. Thick Laminates

The thin laminate results indicate a serious problem with delamination at ply drops in laminates with carbon fiber  $0^\circ$  plies. To better represent actual blade laminates while remaining within the load limits of available testing machines (250 kN), a series of thicker laminates were tested under compression loads only. The number of plies dropped at the same location was varied to simulate unidirectional plies of varying thickness. The laminates are based on the configuration  $[(\pm 45)_3/0_{27}/(\pm 45)_3]$  with additional dropped  $0^\circ$  plies running half of the coupon length, designated  $0^*$ . The  $\pm 45^\circ$  plies are glass/epoxy while the  $0^\circ$  plies are carbon/ epoxy; the next section compares these laminates with all glass laminates having the same configuration and resin.

Figures 6 and 7 give the results for the laminates with varying numbers of plies dropped under the surface  $\pm 45^\circ$  glass plies,  $[(\pm 45)_3/0_n^*/0_{27}/0_n^*/(\pm 45)_3]$ , where  $n$  is 1, 2 or 4. Figure 8 compares the results from the thinner laminates with the thick laminates for the double ply drop case. As expected, the trends in Figures 6 and 7 show lower cycles to delaminate and lower static strength as the number of dropped plies at a location increases. The thick laminate with double ply drops delaminates at about the same strains as do the thin laminates with double ply drops (Figure 8). Thus, little effect of the fraction of  $0^\circ$  plies dropped is evident, indicating that the data should also be representative of still thicker laminates typical of blade spar-caps, and that the  $R=0.1$  and  $-1.0$  data obtained for the thin laminates would also be meaningful for the thick laminates.

The double ply drop data show what may be an unacceptable lifetime decrease for carbon  $0^\circ$  plies, having a total doubled ply thickness of about 0.6 mm. The limited single ply drop results show much improved performance over the double ply drops. Data for single ply drops were difficult to obtain because the load levels for delamination in fatigue were sufficiently close to the ultimate strength that failures occurred in the grips prior to delamination at the ply drop. Taking the data as lower limits to the delamination lifetime, the performance with single (0.3 mm dropped thickness) ply drops appear much less problematic to blade design than do the double ply drops (0.6 mm total dropped thickness).

Earlier work has found only slight effects of the position of the dropped plies through the thickness for static strength.<sup>6,10</sup> Under fatigue loading the  $\pm 45^\circ$  plies which cover the surface  $0^\circ$  ply drops in this laminate configuration may soften considerably in fatigue, providing less constraint on the Mode I peeling of the surface  $0^\circ$ . The effect of dropping  $0^\circ$  plies on the surface of the  $0^\circ$  stack versus the interior is evident in Figure 9 for the double ply drops. The double interior drops appear to perform only slightly better than do the double surface drops at higher cycles. Still, the single surface ply drop performs much better. The single ply drop results in Figure 6 can be compared to literature data for hybrid glass/carbon flexbeams, where single ply drops half as thick as those used here produced delamination at surface strains on the order of 0.5% at  $10^6$  cycles. Thus, the flexbeam data are consistent with the results of this study for a resin system with similar interlaminar toughness.

## C. Glass versus Carbon Fibers

To provide a direct comparison to all glass fiber laminates, the thick laminate configurations for carbon were also tested with glass fiber  $0^\circ$  plies, using the same epoxy resin prepreg. The fiber volume fraction for the glass prepreg was lower than the carbon, 0.47 versus 0.53. As noted earlier (Table 1), the static Mode II delamination resistance was considerably higher for the glass, possibly due to the lower fiber content, which provides thicker resin areas and can produce higher toughness.<sup>14</sup>

The glass results are given in Figures 10 and 11. The data in Figure 10 indicate much higher strains to cause delamination for the glass  $0^\circ$  plies as compared with the carbon. The effects of the number of plies dropped is similar to the carbon  $0^\circ$  case, except for the static data. The relatively high static strength for the 4 ply drop case may reflect an increased buckling resistance provided by the added thickness. Buckling effects are more pronounced with the lower modulus glass in compression. Even with four  $0^\circ$  glass plies dropped at the same location (the surface of the  $0^\circ$  ply stack), the strains to delaminate are similar to those for a single carbon ply drop; the comparison is different when stresses are considered, Figure 11. Now the carbon  $0^\circ$  performance is better than the glass for all cases, but not to the extent of the advantage for glass in terms of strains.

Figures 12 and 13 compare laminates with carbon and glass  $0^\circ$  plies for the double internal ply drop case, which has a less complex delamination pattern than the ply drops at the surface of the  $0^\circ$  stack, which have adjacent  $\pm 45^\circ$  layers. As in other cases, the strains for delamination are much higher for the glass  $0^\circ$  plies, while the stresses are slightly higher for the carbon  $0^\circ$  plies.

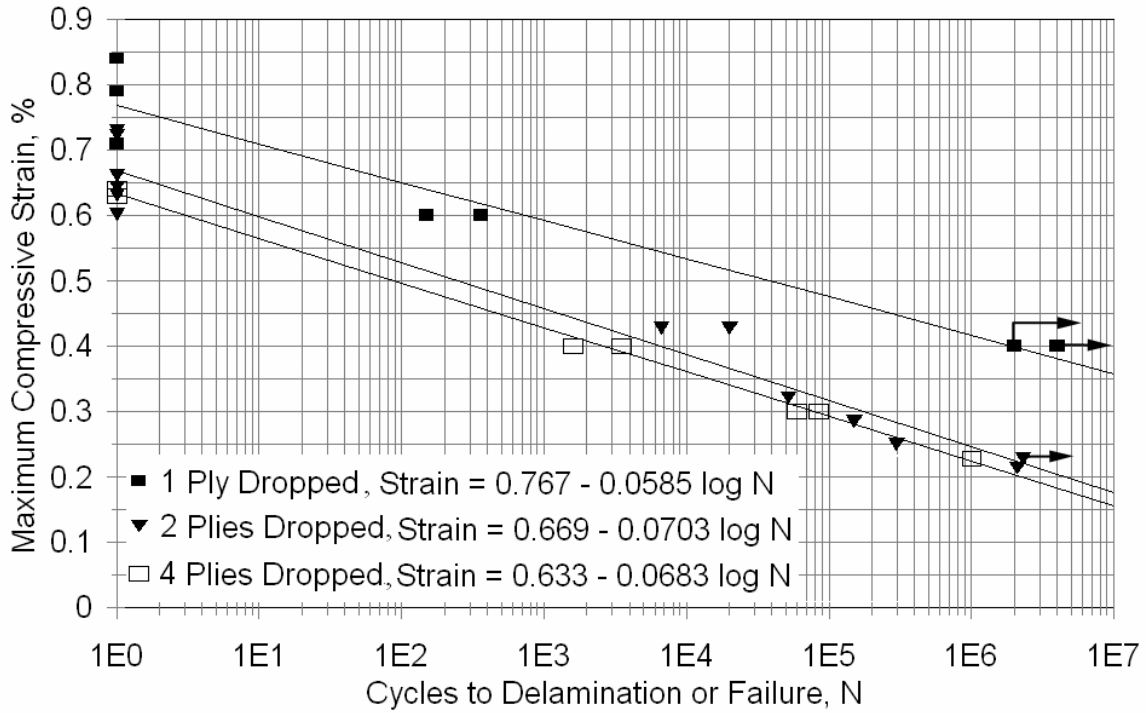


Figure 6. Maximum Compressive Strain versus Cycles to Failure for a  $[(\pm 45)_3/0_n^*/0_{27}/0_n^*/(\pm 45)_3]$  Laminate with  $n = 1, 2$  and  $4$  Plies Dropped at the Surface of the  $0^\circ$  Stack,  $R = 10$  ( $0^\circ$  Plies are Carbon and  $\pm 45^\circ$  Plies are Glass).

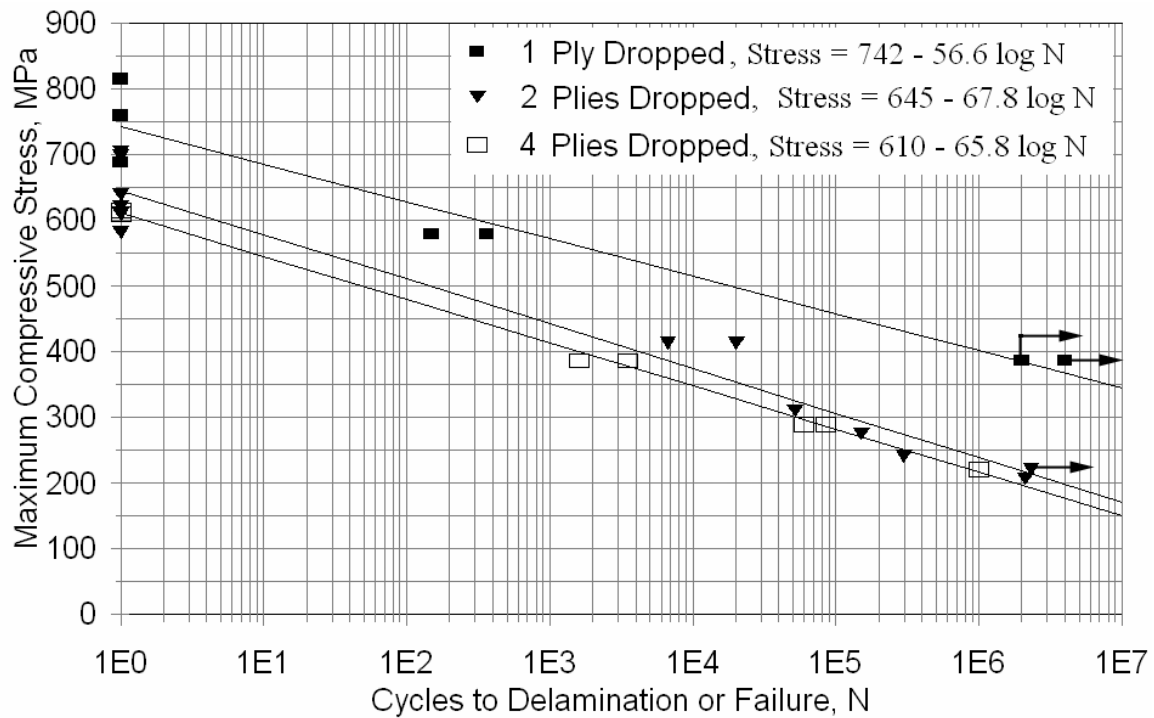


Figure 7. Maximum Compressive Stress versus Cycles to Failure for a  $[(\pm 45)_3/0_n^*/0_{27}/0_n^*/(\pm 45)_3]$  Laminate with  $n = 1, 2$  and  $4$  Plies Dropped at the Surface of the  $0^\circ$  Stack,  $R = 10$  ( $0^\circ$  Plies are Carbon and  $\pm 45^\circ$  Plies are Glass).



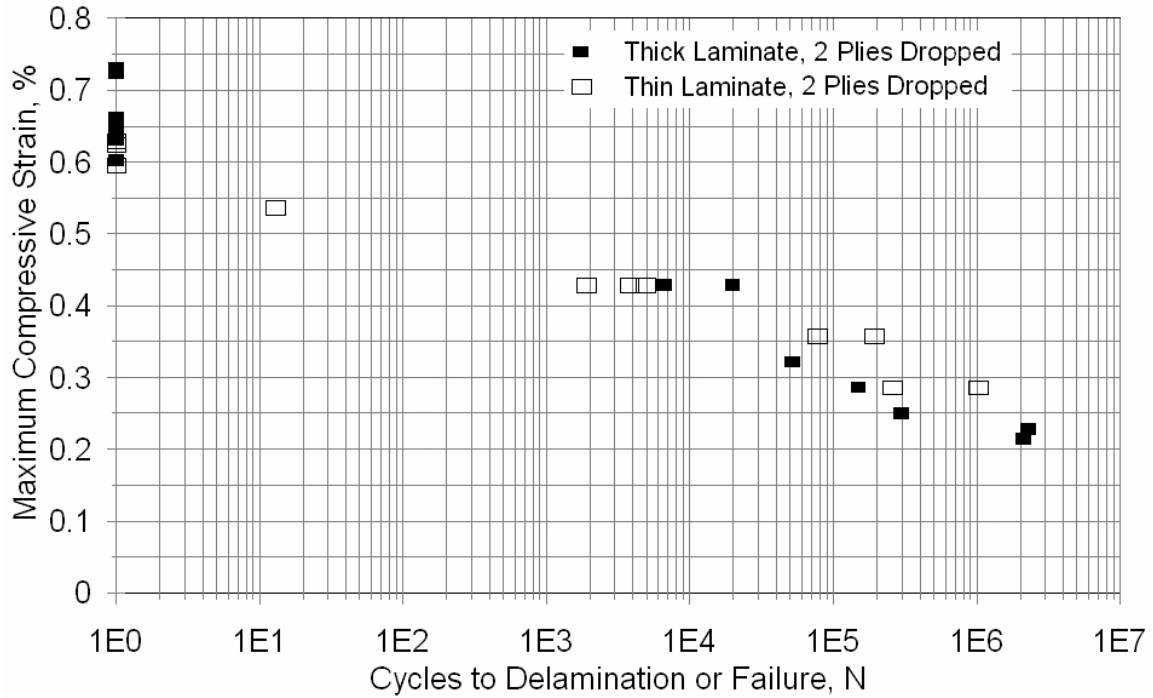


Figure 8. Comparison of Maximum Compressive Strain versus Cycles to Delamination or Failure for a Thick  $[(\pm 45)_3/0_2*/0_{27}/0_2*/(\pm 45)_3]$  Laminate and a Thin  $[(\pm 45)/0_2*/0_9/0_2*/(\pm 45)]$  Laminate, Both with 2 Plies Dropped at the Surface of the  $0^\circ$  Stack ( $0^\circ$  Plies are Carbon and  $\pm 45^\circ$  Plies are Glass).

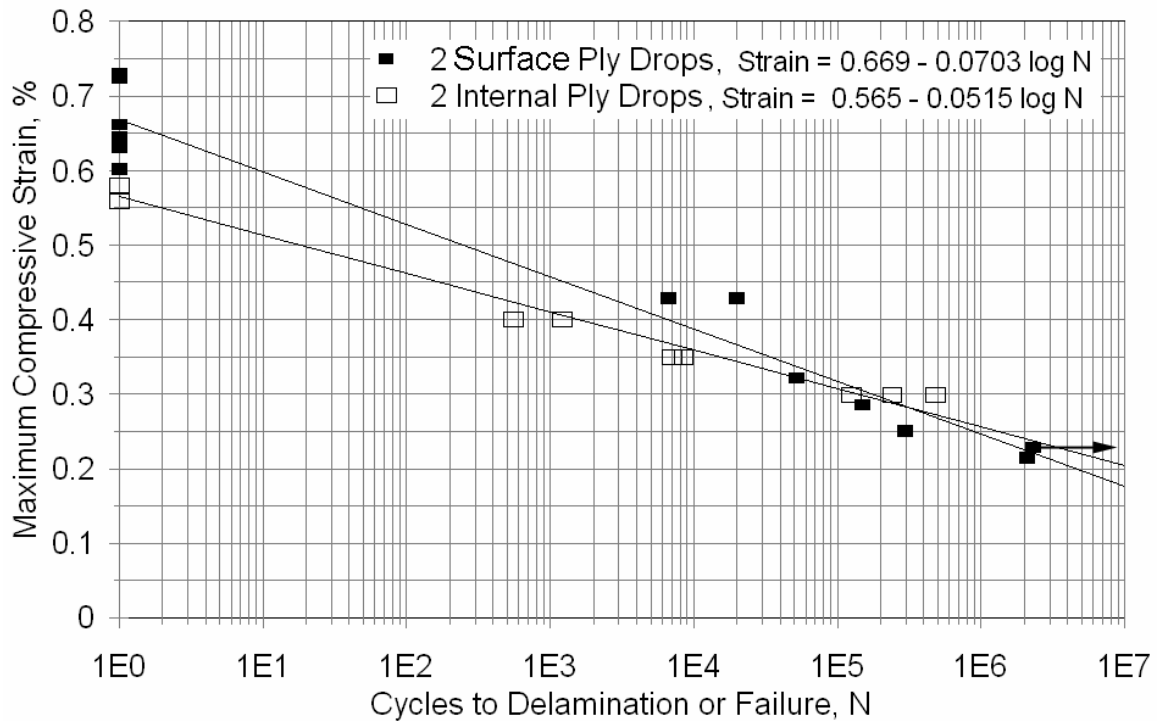


Figure 9. Comparison of the Maximum Compressive Strain versus Cycles to Delamination or Failure for Laminates with Two Plies Dropped at the Surfaces of the  $0^\circ$  Stack  $[(\pm 45)_3/0_2*/0_{27}/0_2*/(\pm 45)_3]$  versus Laminates with Two Internal Plies Dropped at Two Locations  $[(\pm 45)_3/0_9/0_2*/0_9/0_2*/0_9/(\pm 45)_3]$ ,  $R = 10$  ( $0^\circ$  Plies are Carbon and  $\pm 45^\circ$  Plies are Glass).

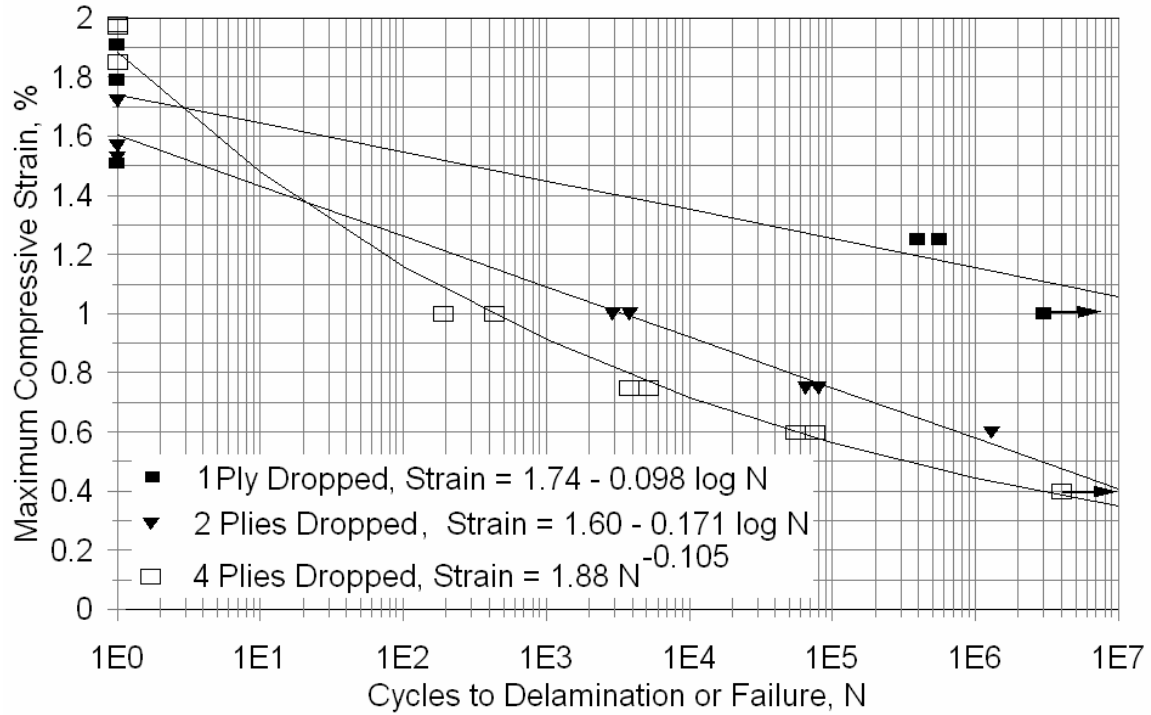


Figure 10. Maximum Compressive Strain versus Cycles to Failure for a  $[(\pm 45)_3/0_n^*/0_{27}/0_n^*/(\pm 45)_3]$  All Glass Laminate with  $n = 1, 2$  and  $4$  Plies Dropped at the Surface of the  $0^\circ$  Stack,  $R = 10$  ( $0^\circ$  and  $\pm 45^\circ$  Plies are Glass).

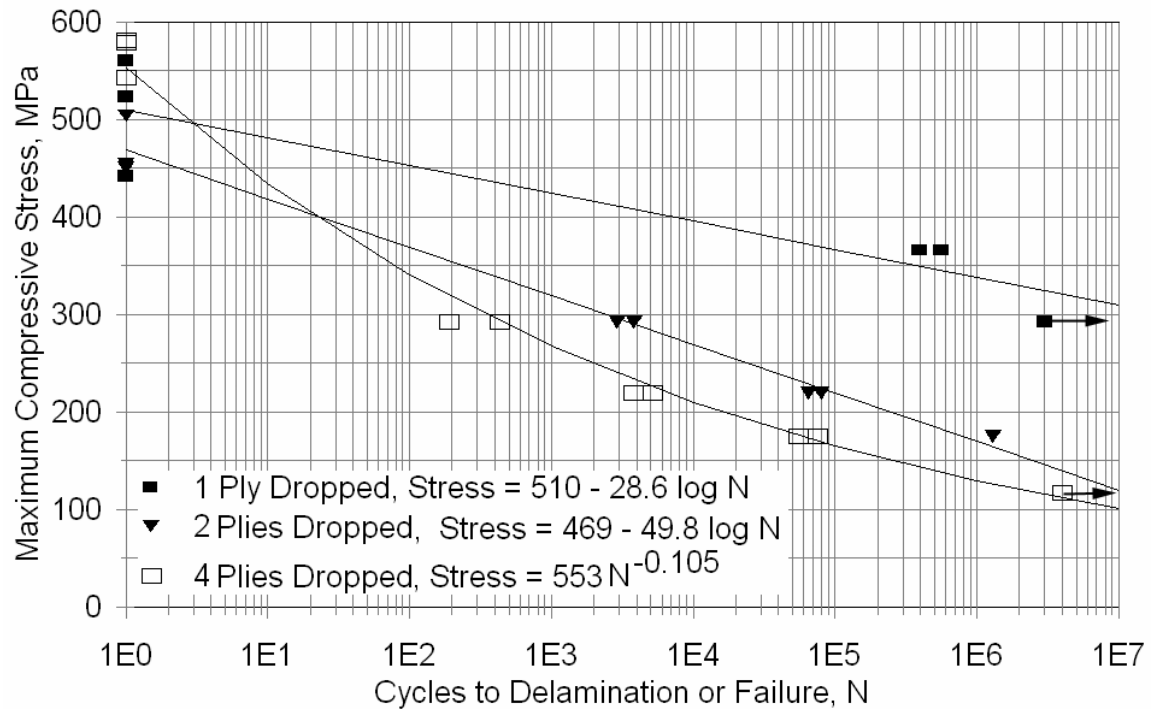


Figure 11. Maximum Compressive Stress versus Cycles to Failure for a  $[(\pm 45)_3/0_n^*/0_{27}/0_n^*/(\pm 45)_3]$  Laminate with  $n = 1, 2$  and  $4$  Plies Dropped at the Surface of the  $0^\circ$  Stack,  $R = 10$  ( $0^\circ$  and  $\pm 45^\circ$  Plies are Glass).

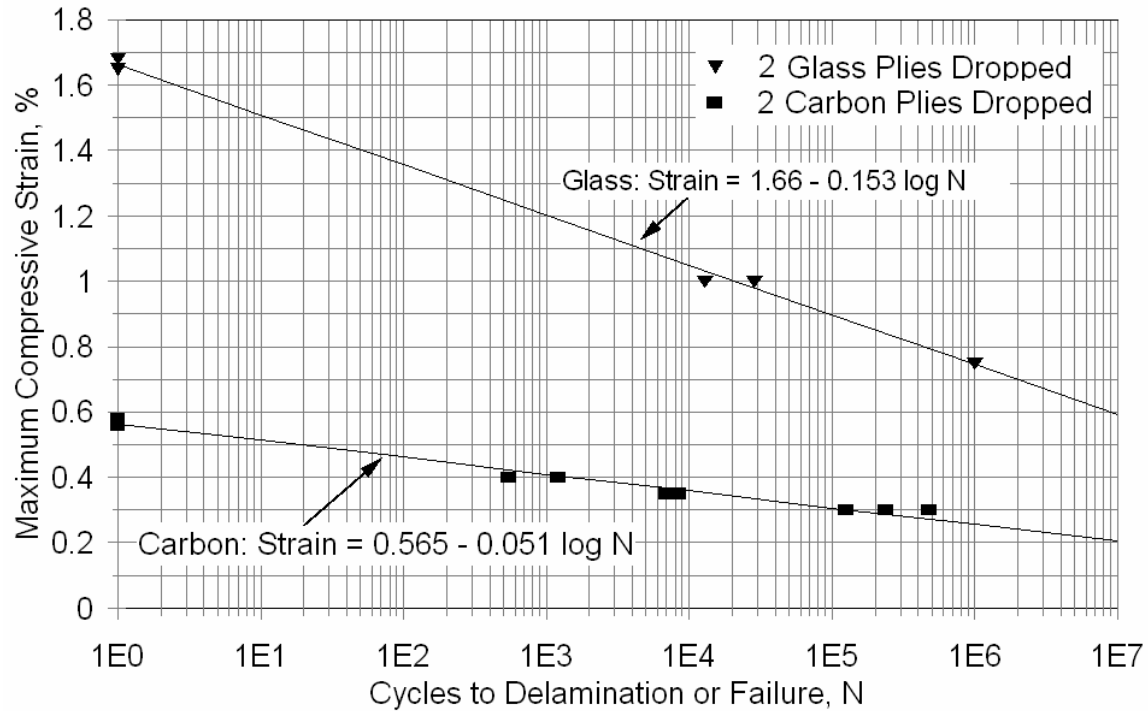


Figure 12. Maximum Compressive Strain versus Cycles to Delaminate with Two Double Internal Ply Drops for Thick Laminates with Carbon and Glass 0° Plies, ±45° Plies are Glass, [(±45)<sub>3</sub>/0<sub>9</sub>/0<sub>2</sub>\*/0<sub>9</sub>/0<sub>2</sub>\*/0<sub>9</sub>/(±45)<sub>3</sub>].

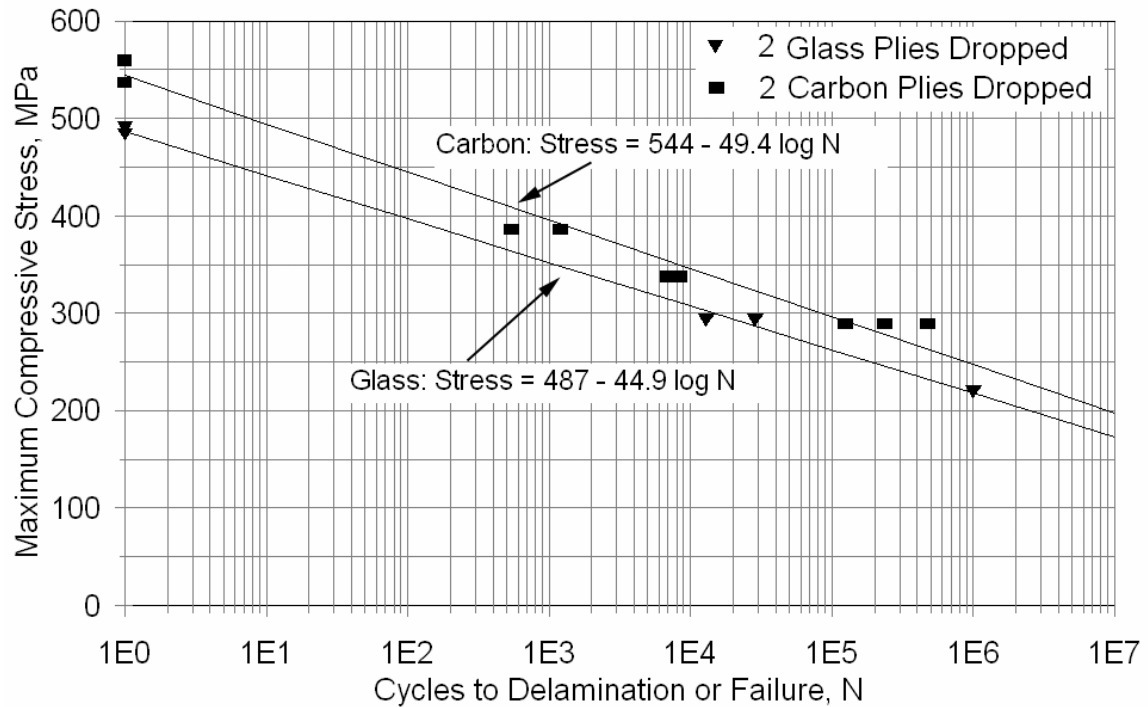


Figure 13. Maximum Compressive Stress versus Cycles to Delaminate with Two Double Internal Ply Drops for Thick Laminates with Carbon and Glass 0° Layers, ±45° Plies are Glass, [(±45)<sub>3</sub>/0<sub>9</sub>/0<sub>2</sub>\*/0<sub>9</sub>/0<sub>2</sub>\*/0<sub>9</sub>/(±45)<sub>3</sub>].

#### D. Discussion

These results indicate that delamination at ply drops under fatigue loading can occur at relatively low applied strain levels for carbon fiber laminates. Delamination at ply drops in glass fiber wind turbine blades has not been widely observed, but has been cited as a factor in a blade failure study.<sup>15</sup> The results of this study indicate potential

problems for ply drops involving ply thickness on the order of 0.6 mm for carbon fibers. This would represent relatively thin plies for infusion processes, but relatively thick plies for prepreg, where most aerospace prepreg ply thicknesses are on the order of 0.15 mm.

The origin of this problem lies mostly in the modulus difference between the carbon and the glass. The higher stresses which operate in carbon fiber materials result in more available strain energy for delamination than for glass, despite their higher elastic modulus. An approximate solution for the total strain energy release rate,  $G_T$ , during delamination of an interior ply of thickness,  $t$ , in very thick laminates, reduces to<sup>6</sup>

$$G_T = \frac{\sigma_C^2 t}{4E_L} = \frac{E_L \varepsilon_C^2 t}{4} \quad (1)$$

where  $\sigma_C$  and  $\varepsilon_C$  are the critical stress and strain in the longitudinal direction at delamination and  $E_L$  is the longitudinal elastic modulus of the dropped ply. This is the strain energy released by the ply as it forms a delamination crack on each surface of the ply.

More detailed finite element analyses indicate that the delamination cracks are predominantly Mode II when growing toward the thick section, but Mode I when growing toward the thin section.<sup>2,8</sup> Reference 5 argues that the initial delamination in fatigue occurs in Mode I. O'Brien<sup>16</sup> argues for consideration primarily of Mode I toughness as dominating delamination problems in composites. However, the thin laminate ply drops in Figures 4 and 5 showed delamination at similar strains for all three loading conditions. Since the Mode I component would change sign in compression versus tension, causing crack closure, this argues for a Mode II domination in these results. A study of Mode II delamination at various R-values by Tanaka and Tanaka<sup>17</sup> found the highest crack growth rates for  $R=-1$ , consistent with Figures 4 and 5; at low maximum  $G_{II}$  values, crack growth rates were insensitive to R-value for the same  $G_{II}$  range.

For the same applied strain,  $\varepsilon$ , the ply stress is higher for the carbon than for glass by the ratio of their longitudinal moduli  $E_C/E_G$ , about 3.5 times for the prepreps used here (Table 1). Thus, from equation (1), the  $G_T$  value driving ply delamination will be about 3.5 times higher for the carbon fibers than for the glass fibers, for the same ply thickness and applied strain. For the same applied stress,  $\sigma$ , the value of  $G_T$  would be about 3.5 times higher for glass due to the lower elastic modulus. These differences would translate into about  $(3.5)^{1/2}$  or 1.9 times higher strain for the same delamination lifetime for glass, or about 1.9 times higher stress for carbon.

Ply drops at the surface of the  $0^\circ$  stack in the present case are difficult to analyze due to the complex response of the  $\pm 45^\circ$  glass overlap plies, which form matrix cracks within the plies as well as the delaminations. The double interior ply drop case provides a simpler delamination pattern, with a delamination growing at each ply interface, effectively unloading the ply as it delaminates. The data in Figures 12 and 13 tend to support Equation (1). In Figure 12, the strain values at the same lifetime for the glass are almost three times higher than for carbon. The stresses, Figure 13, are slightly higher for the carbon, but not close to 1.9 times higher. An additional factor is the lower  $G_{IIc}$  values for the carbon material (Table 1). The actual delaminations are a combination of Modes I and II, and the delamination crack growth rates in pure modes have not yet been determined for these laminates. Other analyses cited above indicate that the main delamination cracks observed in this study, growing toward the thick end, are probably predominantly Mode II. The higher  $G_{IIc}$  value for glass is apparently the reason that the strains are more than 1.9 times higher for glass, while the stresses are less than 1.9 times higher for carbon.

There is no obvious reason for the  $G_{IIc}$  value to be higher for glass fibers than for carbon except that the fiber content is lower for the glass in this particular case. Other direct comparisons between glass and carbon fiber  $G_C$  values for the same resin and process are not known.

If, in general, the  $G_C$  values and  $G$  values for the same fatigue crack growth rate were not sensitive to fiber type, as expected, then at the same applied strain, the carbon would have  $G$  values about 3.5 higher than glass. The strains for equal delamination lifetime would then be about 1.9 times higher for the glass laminate, from Equation (1). This equation also predicts that the  $G_T$  values will be proportional to the dropped thickness,  $t$ , for the same stress. This is consistent with the findings in Reference 2, but the data in Figures 6 and 10 are not separated proportionally in strain to  $E$  as predicted from Equation (1). However, the trends are in the expected order.

## E. Design Implications

It is evident from these results and discussion that, for the same delamination resistance, substantially thicker ply drops can be used for glass than for carbon, in terms of allowable strains. If carbon and glass blades are designed to the same stiffness, then the design strains should be similar if the designs are fatigue sensitive. For carbon, with

excellent in-plane fatigue resistance, ply drop delamination may be a limiting factor unless the plies are very thin, if thickness tapering is used. Manufacturing innovations for rapidly placing thin plies may be important if carbon is to be used in blade structures.

Methodologies for the design and analysis of delamination problems in composites have been validated using finite element analyses.<sup>2,5,7-9</sup> A number of strategies for improving delamination resistance have been demonstrated<sup>6</sup>; the most direct is to increase the resin toughness.<sup>14</sup> However, the resin system used here is already relatively tough compared with other prepregs<sup>14,16</sup> and infusion resins.<sup>12</sup>

## V. Conclusions

The results of this study indicate that ply drops in carbon fiber laminates can lead to ply delamination at relatively low applied strains under fatigue loading. Results were similar for various loading conditions including tension, compression and reversed loading and in compression, for relatively thin and thick laminates. Ply drops involving ply thicknesses of about 0.3 mm had adequate fatigue resistance with carbon fibers, while ply thicknesses of 0.6 mm and greater delaminated at maximum strains of 0.3% and below at one million cycles. By contrast, glass laminates using the same resin and prepreg manufacturing delaminated at strains about three times higher than for carbon; slightly higher stresses were required to delaminate the carbon compared with glass. The results can be understood in terms of the higher elastic modulus of the carbon laminates and the higher delamination resistance measured for the glass in this prepreg system.

## VI. Acknowledgements

This work was funded by Sandia National Laboratories under subcontract Z3609. Prepreg materials were supplied by Newport Adhesives and Composites, Inc. through Mr. Fred Saremi.

## VII. References

- <sup>1</sup>Grimes, G.C. and Dusablon, E.G., "Study of Compression Properties of Graphite/Epoxy Composites with Discontinuities," *Composite Materials: Testing and Design (Sixth Conference)*, ASTM STP 787, I.M. Daniel Ed., American Society for Testing and Materials, Philadelphia, 1982, pp. 513-538.
- <sup>2</sup>Trethewey, B.R., Gillespie, J.W., Jr. and Wilkins., "Interlaminar Performance of Tapered Composite Laminates," *Proceedings of the American Society for Composites, Fifth Technical Conference*, June 11-14, 1990, p. 361.
- <sup>3</sup>Ochoa, O.O., and Chan, W.S., "Tapered Laminates: A Study on Delamination Characterization," *Proceedings of the American Society for Composites, Third Technical Conference*, September 25-29, 1988, p. 633.
- <sup>4</sup>Meirinhos, G., Rucker, J., Cabanac, J-P, Barrau, J-J., "Tapered Laminates Under Static and Fatigue Tension Loading," *Composites Science and Technology*, 62 (2002), pp. 597-603.
- <sup>5</sup>Murri, G.B., Salpekar, S.A., and O'Brien, T.K., "Fatigue Delamination Onset Prediction in Unidirectional Tapered Laminates," *Composite Materials: Fatigue and Fracture (Third Volume)*, ASTM STP 1110, T.K. O'Brian, Ed., American Society for Testing and Materials, Philadelphia, 1991, pp. 312-339.
- <sup>6</sup>Cairns, D.S., Mandell, J.F., Scott, M.E., Maccagnano, J.Z., "Design Considerations for Ply Drops in Composite Wind Turbine Blades," 1997 ASME Wind Energy Symposium, ASME/AIAA, AIAA-97-0953, pp. 197 - 208. (1997).
- <sup>7</sup>Mandell, J.F., Cairns, D.S., Samborsky, D.D., Morehead, R.B., and Haugen, D.J., "Prediction of Delamination in Wind Turbine Blade Structural Details," *Journal of Solar Energy Engineering*, ASME, Vol. 125, No. 4, pp. 522-530. November 2003. (2003).
- <sup>8</sup>Murri, G.B., Schaff, J.R., Dobyns, A.L., "Fatigue Life Analysis of Hybrid Composite Tapered Flexbeams," NASA LaRC Technical Library Digital Repository <http://hdl.handle.net/2002/15079>
- <sup>9</sup>Vizzini, A. J. and Lee, S. W., "Damage Analysis of Composite Tapered Beams," *Journal of the American Helicopter Society*, 40 (2), Apr. 1995, pp. 43-49.
- <sup>10</sup>Avery, D. P., Samborsky D. D., Mandell, J. F. and Cairns, D. S., "Compression Strength of Carbon Fiber Laminates Containing Flaws with Fiber Waviness," 2004 ASME Wind Energy Symposium, ASME/AIAA., AIAA-2004-0174, pp. 54-63, (2004)
- <sup>11</sup>Mandell, J.F., Samborsky, D.D., Wang, L., and Wahl, N.K., "New Fatigue Data for Wind Turbine Blade Materials," *Journal of Solar Energy Engineering*, ASME, Vol. 125, No. 4, pp. 506-514. November 2003.
- <sup>12</sup>Mandell, J.F., Samborsky, D.D., and Cairns, D.S. "Fatigue of Composite Materials and Substructures for Wind Turbine Blades," Contractor Report SAND2002-0771, Sandia National Laboratories, Albuquerque, NM (2002).
- <sup>13</sup>Mandell, J.F., "Fatigue Behavior of Short Fiber Composite Materials," *The Fatigue Behavior of Composite Materials*, K.L. Reifsnider, Ed., Elsevier, Ch. 7, 1991.
- <sup>14</sup>Hunston, D.L., Moulton, R.J., Johnson, N.J., and Bascom, W.D., "Matrix Resin Effects in Composite Delamination: Mode I fracture Aspects," *Toughened Composites*, ASTM STP 937, Norman J. Johnson, Ed., American Society for Testing and Materials, Philadelphia, 1987, pp. 74-94.
- <sup>15</sup>Musial, W., Berry, D., Mandell, J., Ashwill, T., and Hartman, D., "Advances in Blade Design and Material Technology," *Windpower 2005*, American Wind Energy Association, 2005.

<sup>16</sup>O'Brien, T.K., "Composite Interlaminar Shear Fracture Toughness,  $G_{IIc}$ : Shear Measurement or Sheer Myth?," Composite Materials: Fatigue and Fracture, Seventh Volume, ASTM STP 1330, R.B. Bucinell, Ed., American Society for Testing and Materials, Philadelphia, 1998, pp. 3-18.

<sup>17</sup>Tanaka, K., and Tanaka, H., "Stress-Ratio Effect on Mode II Propagation of Interlaminar fatigue Cracks in Graphite/Epoxy Composites," Composite Materials: Fatigue and Fracture (Sixth Volume), ASTM STP 1285, E.A. Armanios, Ed., ASTM, 1997, pp. 126-142.